Magnetic Resonance Imaging–Based Radiomics Models to Predict Early Extrapancreatic Necrosis in Acute Pancreatitis

Ting Zhou, MM,† Chao-lian Xie, MM,* Yong Chen, MD,‡ Yan Deng, MM,† Jia-long Wu, MM,† Rui Liang, MM,† Guo-dong Yang, MM,§ and Xiao-ming Zhang, MD†*

Objective: The aim of the study was to investigate radiomics models based on magnetic resonance imaging (MRI) for predicting early extrapancreatic necrosis (EXPN) in acute pancreatitis.

Methods: Radiomics features were extracted from T2-weighted images of extrapancreatic collections and late arterial-phase images of the pancreatic parenchyma for 135 enrolled patients (94 in the primary cohort, including 47 EXPN patients and 41 in the validation cohort, including 20 EXPN patients). The optimal features after dimension reduction were used for radiomics modeling through a support vector machine. A clinical model, the MR severity index score, and extrapancreatic inflammation on MRI were evaluated.

Results: Twelve optimal features from the extrapancreatic collection images and 10 from the pancreatic parenchyma images were selected for modeling. The pancreatic parenchyma-based and extrapancreatic collection-based radiomics models showed good predictive accuracy in both the training and validation cohorts. The areas under the curve of the extrapancreatic collection-based radiomics model (0.969 and 0.976) were consistent with those of the pancreatic parenchyma-based model (0.931 and 0.921) for both cohorts and better than those of the clinical model and imaging scores for both cohorts.

Conclusions: The MRI-based radiomics models of both the extrapancreatic collections and the pancreatic parenchyma had excellent predictive performance for early EXPN.

Key Words: radiomics, MRI, peripancreatic collection, necrotizing pancreatitis, acute pancreatitis

(*Pancreas* 2021;50: 1368–1375)

Acute pancreatitis (AP) is a common inflammatory disease resulting in potentially serious consequences.[1] Necrotizing pancreatitis is a more severe form with higher rates of infection and mortality.[2,3] The 2012 Revised Atlanta Classification introduced standardized morphologic terms for AP.[3,4] Extrapancreatic necrosis (EXPN) is identified when defined heterogeneous extrapancreatic fat necrosis and liquefied components appear, including EXPN alone and combined necrosis, which accounts for the majority (more than 95%) of cases of necrotizing pancreatitis.[2]

The development of EXPN is closely related to AP severity. Previous studies have reported that extrapancreatic fat lipolysis produces unsaturated fatty acids and adipokines, and unsaturated fatty acid–mediated lipotoxicity causes multiple organ failure, which may further damage the pancreatic parenchymal cells and aggravate the pancreatitis.[5–7] Therefore, it is of great clinical significance to identify potential EXPN cases early and choose the appropriate intervention timing and strategy to improve the patient's prognosis.[6,8]

The identification of morphological changes and complications of AP mainly depend on imaging examinations[8–10]; however, the evolution of extrapancreatic fat necrosis is a dynamic process. In early AP, especially within the first 3 days, the imaging characteristics of EXPN and acute peripancreatic fluid collection (APFC) in interstitial edema pancreatitis are similar, characterized by liquid signals or densities.[11] Interradiologist discrepancies in the description and determination of EXPN in early AP cause challenges in clinical management.[4,12,13]

Compared with computed tomography (CT), magnetic resonance T2-weighted imaging (MR-T2WI) is more accurate in assessing extrapancreatic fluid and fat necrosis debris,[14,15] while T1-weighted imaging is more sensitive for revealing pancreatic or peripancreatic hemorrhage,[16] which suggests that magnetic resonance imaging (MRI) is superior to CT in diagnosing early EXPN.[17] A previous study also showed that MR imaging features of early extrapancreatic changes are helpful in detecting early EXPN[18]; however, this relies on the evaluation of images by radiologists and therefore lacks intrinsic objectivity. Studies have confirmed[5,6] that extrapancreatic fat lipolysis aggravates pancreatic acinar cell damage, resulting in pancreatic perfusion changes. However, in early AP, the changes in pancreatic perfusion are slight and may not be visible on conventional imaging.

Radiomics is a noninvasive technique to extract a mass of potential features invisible to the naked eye on traditional images in a high-throughput manner and to quantitatively analyze these feature data to provide evidence for decision making.[19,20] Previous studies have achieved good results with radiomics models for predicting recurrent pancreatitis and severe pancreatitis.[21,22] Radiomics may be potentially helpful in predicting early EXPN.

Accordingly, in this article, we proposed (1) to establish radiomics models based on MR-T2WI of extrapancreatic collections and MR-enhanced late arterial-phase images of the pancreatic parenchyma to predict early EXPN and (2) to compare the predictive performance of the radiomics models for early EXPN with a clinical model and conventional imaging scoring systems, including the extrapancreatic inflammation on MRI (EPIM) and the MR severity index (MRSI) score.

From the *Department of Radiology, Sichuan Cancer Hospital and Institute, Sichuan Cancer Center, School of Medicine, University of Electronic Science and Technology of China, Chengdu; †Sichuan Key Laboratory of Medical Imaging and Department of Radiology, Affiliated Hospital of North Sichuan Medical College, Nanchong; ‡Department of Radiology, Ruijin Hospital, Shanghai Jiao Tong University School of Medicine, Shanghai; and §Department of Gastroenterology, Affiliated Hospital of North Sichuan Medical College, Nanchong, China.

Received for publication December 3, 2020; accepted October 29, 2021.

Address correspondence to: Xiao-ming Zhang, MD, Sichuan Key Laboratory of Medical Imaging and Department of Radiology, Affiliated Hospital of North Sichuan Medical College, No. 63, Wenhua Rd, Nanchong, Sichuan 637000, China (e-mail: zhangxm@nsmc.edu.cn; cjr.zhxm@vip.163.com).

This study was supported by the National Natural Science Foundation of China (Grant No. 81871440).

The authors declare no conflict of interest.

T.Z., C.X., and Y.C. contributed equally to this work.

Supplemental digital contents are available for this article. Direct URL citations appear in the printed text and are provided in the HTML and PDF versions of this article on the journal's Web site (www.pancreasjournal.com).

Copyright © 2022 Wolters Kluwer Health, Inc. All rights reserved.

DOI: 10.1097/MPA.0000000000001935

Copyright © 2022 Wolters Kluwer Health, Inc. All rights reserved.

MATERIALS AND METHODS

Study Patients

This retrospective study was ethically approved by the local institutional review board, waiving informed consent.

The medical histories of patients admitted to our hospital for first-episode AP from September 2014 to September 2019 were retrospectively analyzed. All enrolled patients underwent routine MR scans and contrast-enhanced MRI within 7 days of onset with extrapancreatic collections visible on MRI and were followed up with either MRI or CT after 7 days or with histopathological findings. Patients with pancreatic carcinoma, chronic consumption, or underlying diseases that may cause peritoneal effusion and those with acute attacks of chronic pancreatitis were excluded. The inclusion and exclusion criteria are detailed in Supplemental Digital Content 1 (http://links.lww.com/MPA/A910). Based on follow-up MRI or CT (evaluated by 2 experienced radiologists, reader 1 and reader 2, with no knowledge of any patient's case history) or histopathological findings, the study patients were classified into an EXPN group and an APFC group. A patient was included in the EXPN group when conforming to 1 of the following 3 criteria: (1) 1 week after onset, follow-up imaging features were in accordance with the diagnosis of EXPN in the 2012 revised Atlanta Classification, showing better defined liquid components and heterogeneous extrapancreatic fat necrosis[23] or an irregular, heterogeneous collection of fluid and necrotic debris with a thick capsule 4 weeks after onset; (2) no significant decrease or even an increase in extrapancreatic collection on follow-up images compared with the initial MRI,[23,24] or (3) histopathologically confirmed extrapancreatic fat necrosis. A patient was included in the APFC group when the extrapancreatic fat exuded slightly with inflammatory changes on follow-up images while fluid collections were basically absorbed, and the pancreas showed a uniform appearance. Any divergences between the 2 radiologists were discussed until agreements were reached. Eventually, a total of 135 AP patients (72 men and 63 women; mean age, 49.8 years [standard deviation, 14.5 years]) were enrolled, including 67 patients with EXPN and 68 with APFC. The median time from onset to initial MR scan was 3 days (range, 1–7 days). All study patients were randomly allocated into a training or a validation cohort at a 7:3 ratio, resulting in 94 patients distributed to the training cohort (47 patients with EXPN and 47 with APFC) and 41 patients distributed to the validation cohort, of whom 20 patients were diagnosed with EXPN. The patient selection flowchart is illustrated in Figure 1.

The case histories of all AP patients were reviewed: etiology, serum calcium and high-sensitivity C-reactive protein (hs-CRP) concentration within 7 days of onset, systemic inflammatory response syndrome (SIRS), length of hospital stay, organ failure, clinical severity in the 2012 revised Atlanta Classification,[3] MRSI,[25] and EPIM scores[26] based on the original enhanced MR.

MR image and CT Scanning

All recruited patients underwent MR scans with a 3.0T system (MR750; GE Medical Systems, Waukesha, Wis) within 1 week of onset. Some patients were followed up 1 week later by CT scans obtained with either a Somatom Definition AS+ 128 (Siemens Healthineers, Forchheim, Germany) or a LightSpeed VCT 128 (GE Healthcare, Fairfield, Conn). For the detailed MRI and CT scan parameters, see Supplemental Digital Content 2 (http://links.lww.com/MPA/A910). All images were acquired in a picture archiving and communication system (PACS).

Image Segmentation and Feature Calculation

The fat-saturated T2W and enhanced late arterial-phase images from the initial MRI were used for feature extraction because the extrapancreatic collections on T2WI were clearer, and the pancreatic parenchyma demonstrated optimal enhancement in the late arterial phase.[27] Two radiologists (reader 3 and reader 4, with 3 and 5 years, respectively, of imaging experience in pancreatitis), without knowledge of the case histories or follow-up results, contoured the largest cross-sections and the upper and lower slices of the extrapancreatic collections manually on the T2W images, as well as the entire pancreatic parenchyma (avoiding bile ducts and peripheral vessels) on every section from the MR-enhanced late arterial-phase images. Image segmentation and feature extraction were performed in IBEX (β1.0, http://bit.ly/IBEX_MDAnderson),

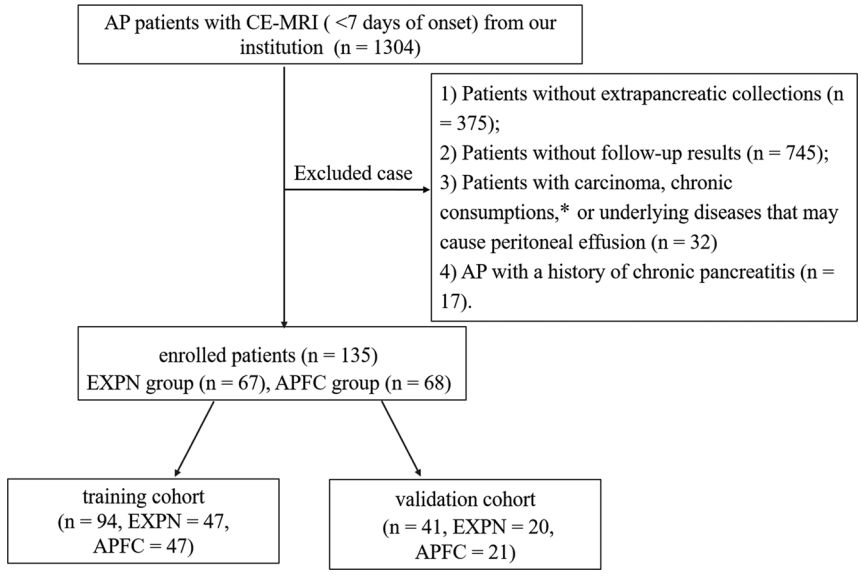

FIGURE 1. Patient selection flowchart. *Chronic consumptions include: (1) various carcinoma, causing cachexia in the patient; (2) other diseases, causing malnutrition in the patient, such as tuberculosis, cirrhosis, and so on, which may cause hypoproteinemia and lead to peritoneal effusion in patients. CE-MRI, contrast-enhanced magnetic resonance image.

© 2022 Wolters Kluwer Health, Inc. All rights reserved.

Copyright © 2022 Wolters Kluwer Health, Inc. All rights reserved.

a MATLAB-based open source software package[28] (Fig. 2). Four groups of radiomics features were extracted: gray-level co-occurrence matrix, gray-level run-length matrix, intensity histogram, and shape, containing a total of 350 features (Supplemental Digital Content 3, http://links.lww.com/MPA/A910). To eliminate the dimensions of the feature magnitudes and to ensure the repeatability of the result, before further analysis, *z*-score normalization was used for feature data preprocessing (Supplemental Digital Content 3, http://links.lww.com/MPA/A910).

Intraobserver and Interobserver Agreement

Reader 3 and reader 4 randomly selected 50 images from the initial fat-saturated T2W and MR-enhanced late arterial-phase images and independently contoured the regions of interest (ROIs) of the extrapancreatic collections and pancreatic parenchyma to assess the interobserver agreement for the radiomics features. Reader 3 contoured these ROIs following the same procedure within a week to evaluate the intraobserver agreement by comparing the newly extracted features with the first extracted features. The intraobserver and interobserver consistency was quantified by the intraclass and interclass correlation coefficients. An interclass correlation coefficient value greater than 0.75 was considered good consistency.[29] Reader 3 completed ROI delineation for all of the remaining images.

Dimension Reduction and Feature Selection

To eliminate the curse of dimensionality and to avoid the occurrence of overfitting during the radiomics modeling, the optimal features were selected in the training cohort as follows. First, according to the distribution and homoscedasticity of the feature data, features with significant differences between the groups were selected by independent sample *t* tests or Mann-Whitney *U* tests. Then, the least absolute shrinkage and selection operator (LASSO), characterized by regularization and variable selection to improve the reliability and predictive accuracy of the radiomics model, was used for dimension reduction to select the optimal features,[30] and the LASSO regression adjusts the model complexity by controlling the regularization parameter (λ) to acquire fewer optimal features for radiomics modeling. In this study, the parameter λ was adjusted through the minimum standard error, and 10-fold cross-validation was used for feature selection to obtain a relatively simple model.

Radiomics Modeling and Verification

Two sets of optimal radiomics features, extracted from the extrapancreatic collections and the MR-enhanced pancreatic parenchyma in the training cohort, were used for radiomics modeling through a support vector machine (SVM) with a Gaussian kernel. The optimal kernel function of the SVM was determined by checking combinations of the kernel size parameter (γ, 0.001–0.1) and the regularized parameter (cost [C], 1–1000) with 10-fold cross-validation. The predictive values of the radiomics models were evaluated by receiver operating characteristic (ROC) curves, and areas under the curve (AUCs). The same radiomics features in the validation cohort were evaluated following the same methods.

Clinical Model and Conventional Imaging Scoring Systems for Predicting Early EXPN

The age, etiology, occurrence of SIRS and serum calcium, and hs-CRP concentrations of each patient were recorded, and a clinical model with these characteristics was established and verified by SVM. The MRSI and EPIM scores based on the original enhanced MR were also evaluated independently by reader 3 and reader 4, and the results from the 2 radiologists were averaged. The AUCs of the clinical model and the EPIM and MRSI scores for the training and validation cohorts were calculated and compared with those from the radiomics models by the DeLong test.

Statistical Analysis

Statistical analysis of the clinical data was performed with the Statistical Package for Social Sciences (SPSS; Version 26.0,

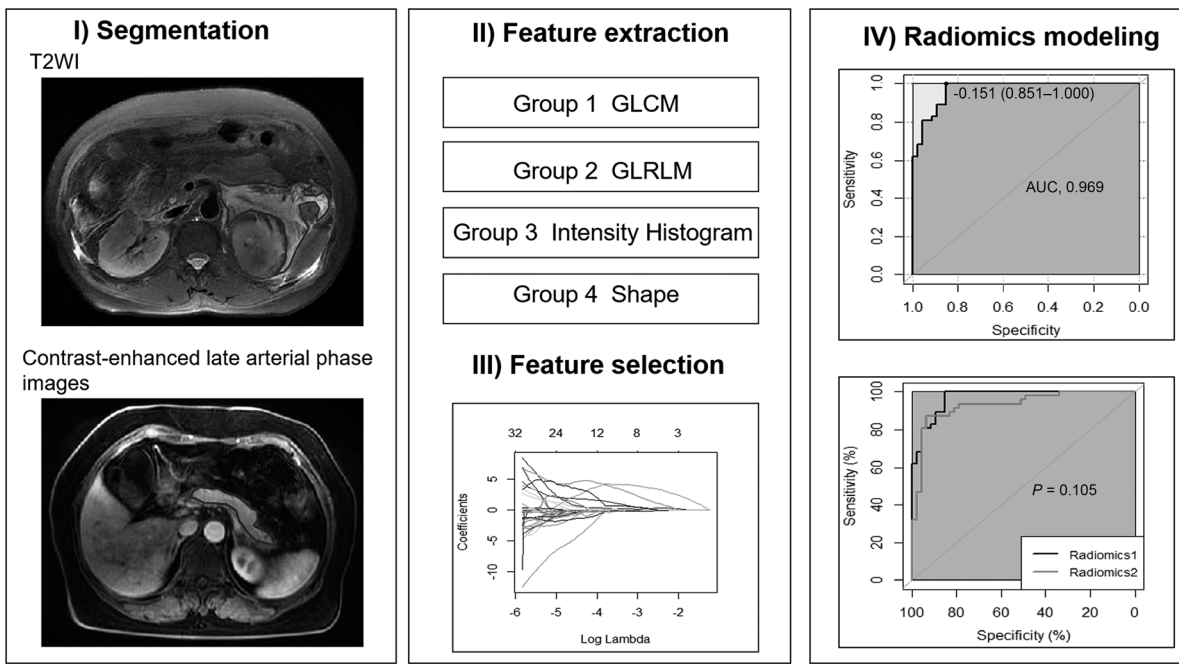

FIGURE 2. Framework for radiomics, including image segmentation, feature extraction and selection, and model building. GLCM, gray-level co-occurrence matrix; GLRLM, gray-level run-length matrix.

© 2022 Wolters Kluwer Health, Inc. All rights reserved.

Copyright © 2022 Wolters Kluwer Health, Inc. All rights reserved.

IBM, Armonk, NY), and analysis of the radiomics features and clinical model was performed with R (v.3.5.2, https://www.r-project.org/, R Foundation, Vienna, Austria). The variables in the primary and validation cohort were statistically analyzed separately. Continuous variables (represented as the means or medians) were compared by independent *t* tests or Mann-Whitney *U* tests, and categorical variables (represented as percentages) were compared by χ^2 test. The "Glmnet" package was used for the LASSO regression, "e1071" was used in SVM modeling, and "pROC" was used to generate and analyze the ROCs. The interradiologist consistency for the imaging scores was assessed by the Wilcoxon rank sum test.

RESULTS

Patient Characteristics

The baseline demographics and characteristics of the 135 AP patients are described in Table 1. Forty-seven patients in the training cohort were diagnosed with EXPN, which was not significantly different from the number of EXPN patients in the validation cohort ($\chi^2 = 0.017$a, $P = 0.607$). All patients were followed up, among which 5 cases were confirmed as EXPN by pathological results, and the remaining cases were confirmed by follow-up images. The median interval to the follow-up scan from the initial MRI for EXPN patients was significantly higher than that for APFC patients in the training cohort ($z = -2.150$, $P = 0.032$). No significant difference was seen between the 2 radiologists in the EPIM or MRSI score by the Wilcoxon test ($P = 0.868$). The presence of SIRS, the serum hs-CRP concentrations, and the EPIM and MRSI scores of the EXPN patients were significantly higher than those of the APFC patients in the training and validation cohorts ($P < 0.05$), whereas the calcium concentration was significantly lower. The length of hospital stay ($P < 0.001$) and the prevalence of severe AP ($P = 0.035$) among EXPN patients were significantly higher than those among APFC patients only in the training cohort. No significant differences were found in organ failure between the 2 groups in either cohort ($P = 0.144$ and 0.111).

Intraobserver and Interobserver Agreement

A total of 350 features in the study were assessed for intraobserver and interobserver agreement. Eventually, 42 features from the extrapancreatic collections and 94 from the pancreatic parenchyma due to poor intraobserver or interobserver agreement were excluded, whereas 308 and 256 features, respectively, were reserved for dimension reduction (see Supplemental Digital Content 4 for details of the process, http://links.lww.com/MPA/A910).

Dimension Reduction, Radiomics Modeling, and Verification

For the T2W images of extrapancreatic collections, 11 features satisfied a Gaussian distribution with homoscedasticity, among which 9 exhibited significant differences between the groups by independent *t* tests. Of the remaining 297 features, 289 showed significant differences by the Mann-Whitney *U* test, resulting in a total of 298 features subjected to LASSO regression. For the MR-enhanced images of the pancreatic parenchyma, 19 of the 20 features with Gaussian distributions and homoscedasticity showed significant differences, whereas 231 features showed significant differences by the Mann-Whitney *U* test; hence, 250 features were subjected to LASSO regression. Finally, LASSO identified the 12 optimal features from the extrapancreatic collection images and 10 from the enhanced pancreatic parenchyma images for SVM modeling, with values of the optimal adjusted parameter λ value of 0.023 and 0.025, respectively, according to the minimum standard error criterion (see Supplemental Digital Content 5 for detailed feature information, http://links.lww.com/MPA/A910).

In this study, the SVM models of both the extrapancreatic collection T2W images and the MR-enhanced pancreatic parenchyma images showed excellent predictive performance in the training cohort (Fig. 3); both had an optimal adjusted γ value of

TABLE 1. Characteristics of Patients With EXPN/APFC in the Training and Validation Cohorts

	Training Cohort (n = 94)			Validation Cohort (n = 41)		
	APFC (n = 47)	EXPN (n = 47)	*P*	APFC (n = 21)	EXPN (n = 20)	*P*
Age, mean (SD), y	49.0 (15.4)	50.6 (13.2)	0.586	50.5 (17.0)	49.4 (13.7)	0.638
Sex, male, n (%)	22 (48.8)	26 (55.3)	0.409	12 (57.1)	12 (60.0)	0.853
Etiology, n (%)			0.524			0.267
Biliary	26 (55.3)	23 (48.9)		11 (52.4)	10 (50.0)	
Hyperlipidemia	14 (29.8)	12 (25.5)		4 (19.0)	8 (40.0)	
Alcohol abuse	1 (2.1)	5 (10.7)		3 (14.3)	1 (5.0)	
Idiopathic	2 (4.3)	3 (6.4)		2 (9.5)	0 (0)	
Other	4 (8.5)	4 (8.5)		1 (4.8)	1 (5.0)	
Follow-up interval, median (range), d	9 (5–60)	12 (5–83)	0.032	12.0 (5–120)	14 (7–60)	0.200
Positive SIRS, n (%)	19 (40.4)	38 (80.9)	0.000	7 (33.3)	13 (65.0)	0.043
OF, n (%)	8 (17.0)	14 (29.8)	0.144	2 (9.5)	7 (35.0)	0.111
POF, n (%)	1 (2.1)	8 (17.0)	0.035	0 (0)	3 (15.0)	0.107*
Length of hospital stay, median (range), d	12.5 (5–32)	18 (6–37)	0.000	13 (6–28)	16.5 (8–43)	0.099
Hs-CRP, median (range), mg/L	62.93 (0.47–275.36)	142.39 (1.64–535.50)	0.000	13.82 (0.38–234.26)	102.74 (13.53–224.63)	0.005
Calcium, mean (SD), mmol/L	2.27 (0.15)	2.05 (0.24)	0.000	2.29 (0.15)	2.12 (0.24)	0.013
MRSI score, median (range)	4 (3–4)	4 (3–10)	0.000	4 (3–4)	5.5 (3−10)	0.000
EPIM score, median (range)	4 (2–7)	7 (4–7)	0.000	5 (1–7)	6.5 (3–7)	0.003

*Fisher exact test.

OF indicates organ failure; POF, persistent organ failure.

© 2022 Wolters Kluwer Health, Inc. All rights reserved.

Copyright © 2022 Wolters Kluwer Health, Inc. All rights reserved.

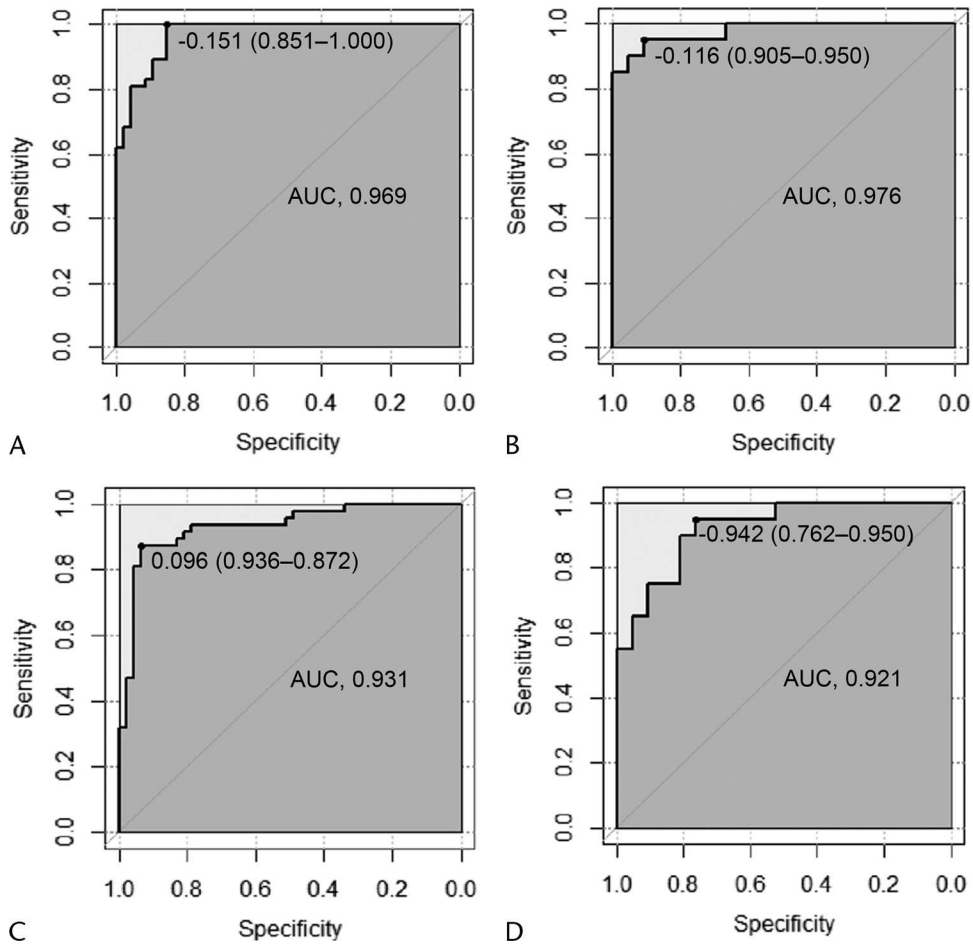

FIGURE 3. A, B, The predictive performance of radiomics models with features from T2W images of extrapancreatic collections in the training cohort (A) and validation cohort (B). C, D, The predictive performance of radiomics model with features from MR-enhanced late arterial-phase images of the pancreatic parenchyma in the training cohort (C) and validation cohort (D).

0.001 and values of C of 10 and 100, respectively, resulting in AUCs for the radiomics models of 0.969 (95% confidence interval [CI], 0.941–0.997) and 0.931 (95% CI, 0.878–0.984), with accuracies of 91.5% and 87.2%, respectively. The predictive values were also good in the validation cohort, demonstrating AUCs for both radiomics models of 0.976 (95% CI, 0.938–1.000) and 0.921 (95% CI, 0.843–0.999), with accuracies of 92.7% and 82.9%, respectively (Table 2).

Predictive Performance of the Clinical Model and Conventional Imaging Scores

The performances of the clinical model and conventional imaging scores are described in Table 2. The SVM clinical model was created with an optimal adjusted γ value of 0.01 and a C value of 10. The AUCs of the clinical model, EPIM score, and MRSI score were 0.856 (95% CI, 0.781–0.931), 0.854 (95% CI, 0.777–0.932), and 0.772 (95% CI, 0.678–0.865), respectively, in the training cohort and 0.771 (95% CI, 0.627–0.916), 0.767 (95% CI, 0.622–0.912), and 0.793 (95% CI, 0.650–0.936) in the validation cohort, with optimal cutoffs of 6 points and 5 points for the EPIM and MRSI score, respectively, in both cohorts.

The radiomics model from the T2W images of the extrapancreatic collection showed the highest accuracy in predicting EXPN in both cohorts. The AUC values of the radiomics model from the MR-enhanced images of the pancreatic parenchyma were not significantly different from those of the radiomics model from the extrapancreatic collections in either cohort ($P = 0.105$ and 0.125, respectively). However, the AUC values of the radiomics model from the extrapancreatic collections in predicting EXPN were significantly better than those of the clinical model and the EPIM and MRSI score in both cohorts ($P < 0.01$; Fig. 4).

DISCUSSION

Our study constructed and verified 2 radiomics models to predict early EXPN based on T2W images of extrapancreatic collections and MR-enhanced late arterial-phase images of the pancreatic parenchyma. The AUCs of the extrapancreatic collection-based radiomics model reached 0.969 and 0.976 in the primary cohort and validation cohort, respectively. Meanwhile, the AUCs of the pancreatic parenchyma-based model also exceeded 0.900. Our results suggest that radiomics provided a more accurate and objective method for identifying early EXPN on MRI, which is of great clinical significance for developing appropriate interventions to improve the prognosis of patients.

In this study, as important indicators for evaluating AP severity,[31–33] the presence of SIRS and serum hs-CRP concentration in EXPN patients were significantly higher than those in APFC patients, and the calcium concentration was significantly

© 2022 Wolters Kluwer Health, Inc. All rights reserved.

Copyright © 2022 Wolters Kluwer Health, Inc. All rights reserved.

TABLE 2. Comparison of Radiomics Models, Clinical Models, and Conventional Imaging Scoring Systems for Predicting EXPN in the Training Cohort and Validation Cohort

	AUC (95% CI)	Accuracy, %	Sensitivity, %	Specificity, %	PPV, %	NPV, %
Training cohort						
Radiomics model 1	0.969 (0.941–0.997)	91.5	97.9	0.85.1	86.8	97.6
Radiomics model 2	0.931 (0.878–0.984)	87.2	87.2	0.87.2	87.2	87.2
Clinical model	0.856 (0.781–0.931)	76.6	72.3	0.80.9	79.1	74.5
EPIM (cutoff ≥6)	0.854 (0.777–0.932)	79.8	87.2	0.72.3	75.9	85.0
MRSI (cutoff ≥5)	0.772 (0.678–0.865)	72.3	44.7	100	100	64.4
Validation cohort						
Radiomics model 1	0.976 (0.938–1.000)	92.7	95.0	0.90.5	90.5	95.0
Radiomics model 2	0.921 (0.843–0.999)	82.9	75.0	0.90.5	88.2	79.2
Clinical model	0.771 (0.627–0.916)	68.3	60.0	76.2	70.6	66.7
EPIM (cutoff ≥6)	0.767 (0.622–0.912)	68.3	75.0	61.9	65.2	72.2
MRSI (cutoff ≥5)	0.793 (0.650–0.936)	78.0	55.0	100	100	70.0

NPV indicates negative predictive value; PPV, positive predictive value; Radiomics 1, radiomics model with features from T2W images of extrapancreatic collections; radiomics 2, radiomics model with features from MR-enhanced late arterial-phase images of pancreatic parenchyma.

lower in EXPN patients, which is consistent with the conclusions of previous studies showing that extrapancreatic necrosis is more severe than interstitial edema pancreatitis.[24,34–36] However, the incidence of severe AP and the length of hospital stay in EXPN patients were significantly higher than those in APFC patients only in the training cohort. No significant differences were seen for organ failure between the 2 groups in either cohort, probably because most of the enrolled patients were moderate-severe patients, whereas severe patients with EXPN without MR examination within 1 week of onset were excluded. This may also be the reason why there were no significant differences in sex, age, or etiology between the patients with EXPN and APFC in either cohort in our study. However, Yang et al[37] reported that age was of great significance for the development of necrotizing pancreatitis. The etiology has also been considered to be associated with AP severity.[38] Therefore, we incorporated age, sex, SIRS, serum calcium, and hs-CRP concentration in the development of the clinical model.

In a previous study evaluating extrapancreatic collections on MRI for early EXPN,[18] the AUCs of the area and range of extrapancreatic collections were 0.871 and 0.803, respectively. Radiomics can extract invisible potential information from conventional images and convert it into feature data that can be quantitatively analyzed, resulting in objective and accurate decision making. In this study, T2W images showing clear extrapancreatic collections (extrapancreatic fluid or necrosis) were selected for feature extraction. The results demonstrated that the predictive

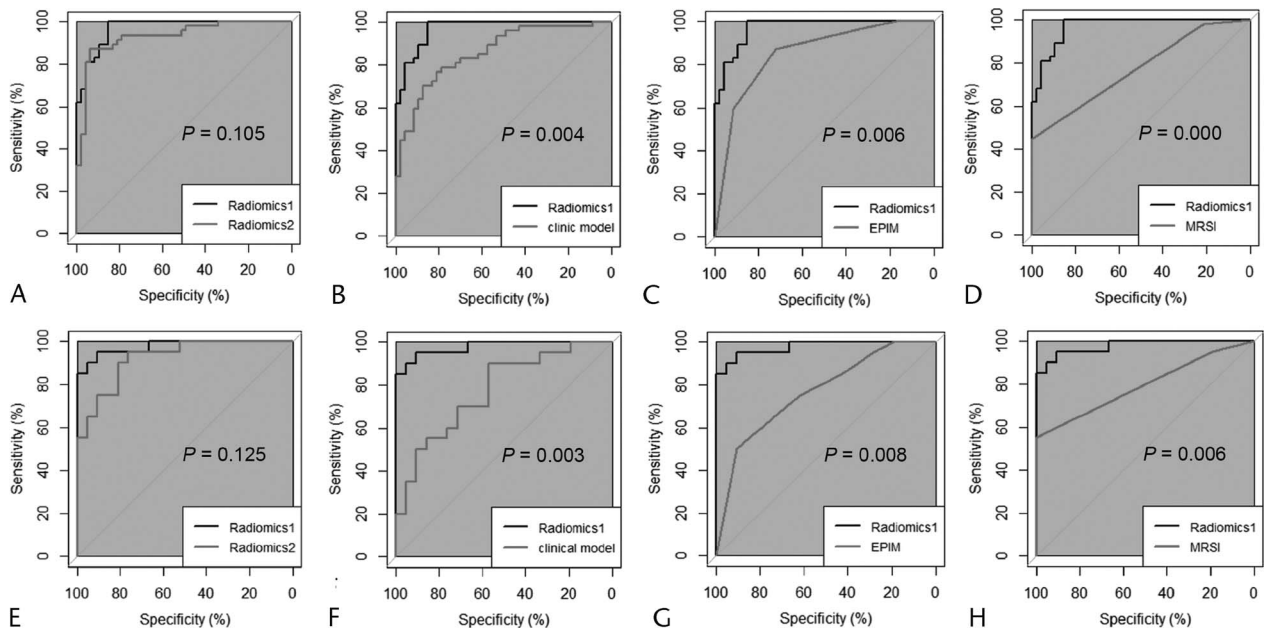

FIGURE 4. The AUC comparison of radiomics model 1 with radiomics model 2, clinical model, EPIM score, and MRSI score in the training cohort (A–D) and validation cohort (E–H). Radiomics 1, radiomics model with features from T2W images of extrapancreatic collections; radiomics 2, radiomics model with features from MR-enhanced late arterial-phase images of the pancreatic parenchyma.

© 2022 Wolters Kluwer Health, Inc. All rights reserved.

Copyright © 2022 Wolters Kluwer Health, Inc. All rights reserved.

performance of the T2W images of the extrapancreatic collection-based radiomics model for early EXPN was the highest, with the AUCs of both the training and validation cohorts greater than 0.950, better than the predictive performance of the morphology of extrapancreatic collections on T2WI.[18] Our results indicated that radiomics provided a more accurate and objective method for identifying early EXPN from MRI.

During a pancreatitis attack, pancreatic acinar cells are damaged, and the microcirculation is altered. Then, trypsin is secreted from the basolateral into the extracellular area,[39] which works together with inflammatory mediators to cause a series of complications and extrapancreatic fat necrosis. Fat cell lipolysis produces unsaturated fatty acids and adipokines, which further aggravate the extrapancreatic adipocyte and pancreatic acinar cell damage.[5,6] Pancreatic parenchymal injury is closely associated with EXPN. Therefore, we speculated that early pancreatic perfusion changes could reflect EXPN. A previous study applied radiomics to explore early potential pancreatic parenchymal changes to predict severe AP, with good performance.[22] Our study also established a radiomics model from MR-enhanced images to evaluate early changes in the pancreatic parenchyma and to predict early EXPN. The results showed that the predictive value of the pancreatic parenchyma-based radiomics model was high and comparable to that of the extrapancreatic collection-based model. Our results further confirmed that pancreatic parenchymal injury is closely associated with EXPN.

A previous study evaluated extrapancreatic inflammation and pancreatic perfusion on MRI and found that the EPIM and MRSI scores were helpful in identifying early EXPN.[18] This study also found similar results, but the AUCs of the EPIM and MRSI scores were significantly lower than those of the T2W images of the extrapancreatic collection-based radiomics model and lower than those of the MR-enhanced pancreatic parenchyma-based model. This is because in early pancreatitis, pancreatic parenchyma injury and extrapancreatic inflammation are in progress, and the parenchyma changes are slight and may not be visible to the naked eye. Moreover, the performance of conventional imaging features often lags behind disease progression, making it more difficult to observe. The evaluation of extrapancreatic inflammation is subjective and culminates in an underestimation of EXPN.

Several limitations existed in our study. First, the use of a single center for the study may lead to some difficulty in generalizing the imaging methods to other centers. Second, although we prospectively followed the patients with MRI or CT, the sample size was still small, and some critical and mild patients were excluded without MR examination within 1 week of onset, which may lead to no significant differences in some results due to underpowering. Third, the follow-up interval for patients was relatively random, whereas the follow-up interval of EXPN patients in the validation cohort was longer than that of the APFC patients, probably because the EXPN patients had a more serious condition. The EXPN patients were followed up repeatedly to ensure that there was little impact on the diagnosis of EXPN.

In conclusion, the radiomics models of the T2W images of extrapancreatic collections and the MR-enhanced images of the pancreatic parenchyma had excellent predictive performance for early EXPN in AP. Radiomics, as a quantitative method, provides a more accurate and objective method to use MRI to identify early EXPN, further confirming that pancreatic parenchymal injury is closely associated with the development of EXPN.

ACKNOWLEDGMENTS

The first author would like to thank my supervisor Professor Zhang Xiaoming who helped me during the design and writing of the thesis. In addition, the authors thank the teachers in our Department of Radiology and Gastroenterology for their help with this study. The authors thank Ms Zhu Tao from the Department of Preventive Medicine for guiding the statistical analysis in this study.

REFERENCES

1. Forsmark ChE, Vege SS, Wilcox CM. Acute pancreatitis. *N Engl J Med*. 2017;376:598–599.
2. Chua TY, Walsh RM, Baker ME, et al. Necrotizing pancreatitis: diagnose, treat, consult. *Cleve Clin J Med*. 2017;84:639–648.
3. Banks PA, Bollen TL, Dervenis C, et al. Classification of acute pancreatitis—2012: revision of the Atlanta classification and definitions by international consensus. *Gut*. 2013;62:102–111.
4. Badat N, Millet I, Corno L, et al. Revised Atlanta classification for CT pancreatic and peripancreatic collections in the first month of acute pancreatitis: interobserver agreement. *Eur Radiol*. 2019;29:2302–2310.
5. Durgampudi C, Noel P, Patel K, et al. Acute lipotoxicity regulates severity of biliary acute pancreatitis without affecting its initiation. *Am J Pathol*. 2014;184:1773–1784.
6. Noel P, Patel K, Durgampudi C, et al. Peripancreatic fat necrosis worsens acute pancreatitis independent of pancreatic necrosis via unsaturated fatty acids increased in human pancreatic necrosis collections. *Gut*. 2016;65:100–111.
7. Karpavicius A, Dambrauskas Z, Gradauskas A, et al. The clinical value of adipokines in predicting the severity and outcome of acute pancreatitis. *BMC Gastroenterol*. 2016;16:99.
8. Shyu JY, Sainani NI, Sahni VA, et al. Necrotizing pancreatitis: diagnosis, imaging, and intervention. *Radiographics*. 2014;34:1218–1239.
9. Xiao B, Xu HB, Jiang ZQ, et al. Current concepts for the diagnosis of acute pancreatitis by multiparametric magnetic resonance imaging. *Quant Imaging Med Surg*. 2019;9:1973–1985.
10. Murphy KP, O'Connor OJ, Maher MM. Updated imaging nomenclature for acute pancreatitis. *AJR Am J Roentgenol*. 2014;203:W464–W469.
11. Manikkavasakar S, AlObaidy M, Busireddy KK, et al. Magnetic resonance imaging of pancreatitis: an update. *World J Gastroenterol*. 2014;20:14760–14777.
12. Bouwense SA, van Brunschot S, van Santvoort HC, et al. Describing peripancreatic collections according to the revised Atlanta classification of acute pancreatitis: an international interobserver agreement study. *Pancreas*. 2017;46:850–857.
13. Sternby H, Verdonk RC, Aguilar G, et al. Significant inter-observer variation in the diagnosis of extrapancreatic necrosis and type of pancreatic collections in acute pancreatitis—an international multicenter evaluation of the revised Atlanta classification. *Pancreatology*. 2016;16:791–797.
14. Sun H, Zuo HD, Lin Q, et al. MR imaging for acute pancreatitis: the current status of clinical applications. *Ann Transl Med*. 2019;7:269.
15. Zaheer A, Singh VK, Qureshi RO, et al. The revised Atlanta classification for acute pancreatitis: updates in imaging terminology and guidelines. *Abdom Imaging*. 2013;38:125–136.
16. Tang MY, Chen TW, Bollen TL, et al. MR imaging of hemorrhage associated with acute pancreatitis. *Pancreatology*. 2018;18:363–369.
17. Tang MY, Chen TW, Huang XH, et al. Acute pancreatitis with gradient echo T2*-weighted magnetic resonance imaging. *Quant Imaging Med Surg*. 2016;6:157–167.
18. Zhou T, Tang MY, Deng Y, et al. MR imaging for early extrapancreatic necrosis in acute pancreatitis. *Acad Radiol*. 2021;28(suppl 1):S225–S233.
19. Lambin P, Rios-Velazquez E, Leijenaar R, et al. Radiomics: extracting more information from medical images using advanced feature analysis. *Eur J Cancer*. 2012;48:441–446.

© 2022 Wolters Kluwer Health, Inc. All rights reserved.

Copyright © 2022 Wolters Kluwer Health, Inc. All rights reserved.

20. Lambin P, Leijenaar RTH, Deist TM, et al. Radiomics: the bridge between medical imaging and personalized medicine. *Nat Rev Clin Oncol*. 2017;14: 749–762.
21. Chen Y, Chen TW, Wu CQ, et al. Radiomics model of contrast-enhanced computed tomography for predicting the recurrence of acute pancreatitis. *Eur Radiol*. 2019;29:4408–4417.
22. Lin Q, Ji YF, Chen Y, et al. Radiomics model of contrast-enhanced MRI for early prediction of acute pancreatitis severity. *J Magn Reson Imaging*. 2020;51:397–406.
23. Bollen TL, Singh VK, Maurer R, et al. A comparative evaluation of radiologic and clinical scoring systems in the early prediction of severity in acute pancreatitis. *Am J Gastroenterol*. 2012;107:612–619.
24. Bakker OJ, van Santvoort H, Besselink MG, et al. Extrapancreatic necrosis without pancreatic parenchymal necrosis: a separate entity in necrotising pancreatitis? *Gut*. 2013;62:1475–1480.
25. Tang W, Zhang XM, Xiao B, et al. Magnetic resonance imaging versus Acute Physiology And Chronic Healthy Evaluation II score in predicting the severity of acute pancreatitis. *Eur J Radiol*. 2011;80: 637–642.
26. Zhou T, Chen Y, Wu JL, et al. Extrapancreatic inflammation on magnetic resonance imaging for the early prediction of acute pancreatitis severity. *Pancreas*. 2020;49:46–52.
27. Kanematsu M, Shiratori Y, Hoshi H, et al. Pancreas and peripancreatic vessels: effect of imaging delay on gadolinium enhancement at dynamic gradient-recalled-echo MR imaging. *Radiology*. 2000;215:95–102.
28. Zhang L, Fried DV, Fave XJ, et al. IBEX: an open infrastructure software platform to facilitate collaborative work in radiomics. *Med Phys*. 2015;42: 1341–1353.
29. Sullivan DC, Obuchowski NA, Kessler LG, et al. Metrology standards for quantitative imaging biomarkers. *Radiology*. 2015;277:813–825.
30. Huang YQ, Liang CH, He L, et al. Development and validation of a radiomics nomogram for preoperative prediction of lymph node metastasis in colorectal cancer. *J Clin Oncol*. 2016;34:2157–2164.
31. He WH, Zhu Y, Zhu Y, et al. Comparison of multifactor scoring systems and single serum markers for the early prediction of the severity of acute pancreatitis. *J Gastroenterol Hepatol*. 2017;32:1895–1901.
32. Khanna AK, Meher S, Prakash S, et al. Comparison of Ranson, Glasgow, MOSS, SIRS, BISAP, APACHE-II, CTSI scores, IL-6, CRP, and procalcitonin in predicting severity, organ failure, pancreatic necrosis, and mortality in acute pancreatitis. *HPB Surg*. 2013;2013:367581.
33. Vasudevan S, Goswami P, Sonika U, et al. Comparison of various scoring systems and biochemical markers in predicting the outcome in acute pancreatitis. *Pancreas*. 2018;47:65–71.
34. Sharma V, Rana SS, Bhasin DK. Extra-pancreatic necrosis alone: contours of an emerging entity. *J Gastroenterol Hepatol*. 2016;31:1414–1421.
35. Sakorafas GH, Tsiotos GG, Sarr MG. Extrapancreatic necrotizing pancreatitis with viable pancreas: a previously under-appreciated entity. *J Am Coll Surg*. 1999;188:643–648.
36. Dirweesh A, Khan MY, Li Y, et al. Isolated peripancreatic necrosis (PPN) is associated with better clinical outcomes compared with combined pancreatic and peripancreatic involvement (CPN)—a systematic review and meta-analysis. *Pancreatology*. 2020;20:1–8.
37. Yang DD, Zuo HD, Wu CQ, et al. The characteristics of acute necrotizing pancreatitis in different age stages: an MRI study. *Eur J Radiol*. 2020; 122:108752.
38. Zhu Y, Pan X, Zeng H, et al. A study on the etiology, severity, and mortality of 3260 patients with acute pancreatitis according to the revised Atlanta Classification in Jiangxi, China over an 8-year period. *Pancreas*. 2017;46: 504–509.
39. Lee PJ, Papachristou GI. New insights into acute pancreatitis. *Nat Rev Gastroenterol Hepatol*. 2019;16:479–496.

© 2022 Wolters Kluwer Health, Inc. All rights reserved.

Copyright © 2022 Wolters Kluwer Health, Inc. All rights reserved.